Magnetic properties of iron-rich Fe-Sc glasses

D. H. Ryan, J. O. Ström-Olsen, and W. B. Muir
Physics Department, McGill University, Montreal, Quebec, Canada H3A 2T8

J. M. Cadogan* and J. M. D. Coey
Department of Pure and Applied Physics, Trinity College, Dublin 2, Ireland
(Received 10 August 1988; revised manuscript received 10 July 1989)

Amorphous Fe_xSc_{100-x} alloys with $x=89$, 90, and 91, prepared by melt spinning, exhibit a single sharp spin-freezing transition at 100±3 K to an asperomagnetic state. The average ^{57}Fe hyperfine field at 4.2 K is 22.7 T. Magnetization curves indicate that fields in excess of 20 T would be required to achieve saturation at 4.2 K and that the iron moment extrapolated to infinite field is $1.6\mu_B$. Hysteresis is found at low temperatures. On hydrogenation, the alloys become soft collinear ferromagnets with an iron moment of $2.2\mu_B$ and a Curie point of 310 K. A magnetic phase diagram is presented that summarizes the magnetic properties of a-Fe_xM_{100-x} systems (M =Sc, Y, Zr, or Hf). The behavior when M is a IIIb element (Sc,Y) is distinct from that when it is a IVb element (Zr,Hf), suggesting that the direct iron-iron exchange is frustrated by an indirect antiferromagnetic coupling in the IIIb alloys. Both groups tend to a common limit as $x \rightarrow 100$.

INTRODUCTION

The magnetic properties of iron-rich amorphous Fe_xM_{100-x} alloys (where M is an early transition metal: Sc, Y, Zr, or Hf) have been a source of interest and controversy for several years. They allow an approach to pure amorphous iron in a controlled manner, and inference of its magnetic properties by extrapolation.[1-3] At low iron concentrations ($x<40$) all of the systems studied behave in a similar manner; an iron moment appears inhomogeneously at $x\sim35$ and the materials exhibit random noncollinear, or spin-glass-like order with $T_c \leq 30$ K.[1] As x is increased, the magnetic behavior develops in two distinct ways, depending on the alloying element. For M = Zr (Ref. 4) and Hf (Ref. 5), the alloys become ferromagnetic with T_c rising to ~ 300 K. Above $x\sim80$, T_c starts to fall again and the alloys exhibit random, noncollinear or asperomagnetic order[6] with greatly reduced ordering temperatures. No reduction in iron moment accompanies the fall in T_c; it remains essentially constant in this concentration range. A second, transverse spin-freezing transition has been observed below T_c in iron-rich a-Fe-Zr (Refs. 7 and 8) and a-Fe-Hf (Ref. 9) alloys. This behavior has been interpreted in terms of a ferromagnetic spin-glass model[3,8,10] and results from competing positive and negative exchange. By contrast, alloys with Y are never ferromagnetic; they are asperomagnets with $T_c \leq 100$ K for all $x>40$.[11,12] A single, broad, spin-freezing transition is observed.

The first report on melt-spun amorphous $Fe_{90}Sc_{10}$ by Day *et al.*[13] shows an ordering temperature of 99 K and an average hyperfine field of 22.9 T at 4.2 K. This lead us to anticipate magnetic behavior similar to that of amorphous alloys of iron with yttrium (the group IIIb element directly below Sc in the periodic table), although the iron moment in alloys with scandium appears somewhat smaller than with yttrium. On the other hand, Fukamichi *et al.*[14] prepared a series of thick foils by dc sputtering ($67 \leq x \leq 90$) and found the magnetic behavior to be almost the same as amorphous Fe-Zr, with moments ~20% larger than in a-Fe-Zr, and an ordering temperature of ~200 K for $Fe_{90}Sc_{10}$.

Here we report a more extensive study of the magnetic properties of a-Fe_xSc_{100-x} ($x=89$, 90, and 91) combining dc magnetization measurements and Mössbauer spectroscopy. We include an account of the effects of hydrogen, and relate the results to our earlier work on iron-rich amorphous alloys with Zr,[8] Hf,[9] and Y.[15] Although Y and Sc are somewhat different chemically, as is shown for example by different moments iron holds in each, the magnetic properties of amorphous Fe_xSc_{100-x} alloys are very close to those of their Y analogs, which we believe reflects the fact that both IIIb elements permit indirect coupling between distant local moments.

SAMPLE PREPARATION AND CHARACTERIZATION

Alloys were prepared by arc-melting appropriate quantities of Fe (99.99%) and Sc (99.9%) under titanium-gettered argon. The alloys were melt-spun on a copper wheel with a tangential speed of 50 m/s under high-purity helium. Meter-length ribbons of a-Fe_xSc_{100-x} were obtained for $x=89$, 90 and 91. Alloys outside this range could not be made without some precipitated α-Fe. The absence of crystallinity was confirmed by x-ray diffraction with Cu K_α radiation [Figure 1(a)], and by thermogravimetric analysis (TGA) in the presence of a magnetic field gradient. Since the crystallization products (α-Fe and Fe_2Sc) are both magnetic, TGA allows us to put an upper bound of 0.1% on crystalline precipitates. Sample composition was checked by electron mi-

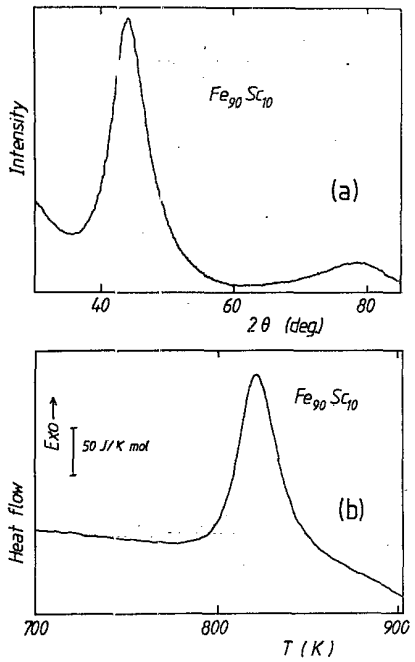

FIG. 1. (a) X-ray diffraction pattern for a-$Fe_{90}Sc_{10}$. (b) DSC scan for a-$Fe_{90}Sc_{10}$ at 40 K/min showing the crystallization exotherm at 822 K.

croprobe analysis and found to be within 0.2 at. % of the nominal value in all cases.

Crystallization was studied by differential scanning calorimetry (DSC) using a Perkin Elmer DSC-2C. All compositions exhibit a single exotherm at ~800 K [Fig. 1(b)], forming α-Fe and Fe_2Sc (both λ_1 and λ_2 phases were seen)[16].

Magnetic properties were studied by magnetization measurements up to 5 T with a vibrating-sample magnetometer and up to 19 T at the Service National des Champs Intenses, Grenoble with an extraction magnetometer. Mössbauer spectra were collected on a conventional constant-acceleration spectrometer with a 1-GBq $^{57}CoRh$ source. These systems can be operated from 4.2 to 300 K. Room-temperature Mössbauer spectra show no sign of magnetic ordering and consist of broad, asymmetric doublets which are well fitted assuming a linear correlation between isomer shift (δ, relative to α-Fe) and quadrupole splitting (Δ), with average values $\langle\delta\rangle=-0.09$ mm/s, and $\langle\Delta\rangle=0.40$ mm/s (Fig. 3).

Hydrogen charging was achieved electrolytically.[17] The saturated hydrogen content corresponds to an [H]/[Sc] ratio of approximately 3. Thermopiezic analysis (TPA) on an instrument designed specially to study milligram samples[18] was used to determine hydrogen content and examine desorption characteristics. The bulk of the absorbed hydrogen is lost below 200 °C (Fig. 2).

RESULTS

Mössbauer spectra measured at 4.2 K (Fig. 3) show the broad distribution of hyperfine fields typical of magnetically ordered amorphous alloys. Average hyperfine fields, and corresponding iron moments (using a conversion factor of 15 T/μ_B as found in α-Fe and crystalline Fe-Y alloys[19]) are given in Table I. Magnetization curves at 4.2 K do not saturate in fields of up to 19 T, remaining well below the values expected from the moments deduced from the average hyperfine fields. However, the moment M_∞ obtained by extrapolating to $1/H=0$ does match that given by the hyperfine field. Magnetization curves are shown in Fig. 4. Hysteresis appears in the liquid-helium temperature range. Values of remanence M_r and coercivity $\mu_0 H_c$ at 4.2 K are included in Table I, together with the site averages $\langle B_{hf}\rangle$, M_∞, and M_z. M_z,

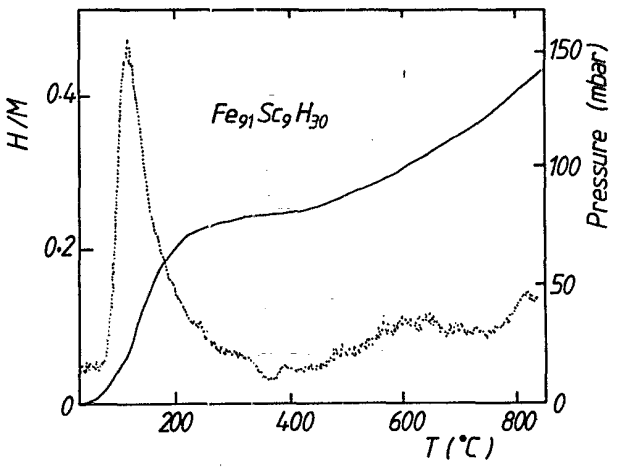

FIG. 2. Thermopiezic analysis (TPA) of hydrogenated a-$Fe_{91}Sc_9H_{30}$ showing hydrogen desorption on heating at 15 °C/min in vacuum. The dotted curve is the derivative (dP/dT) of the heating curve.

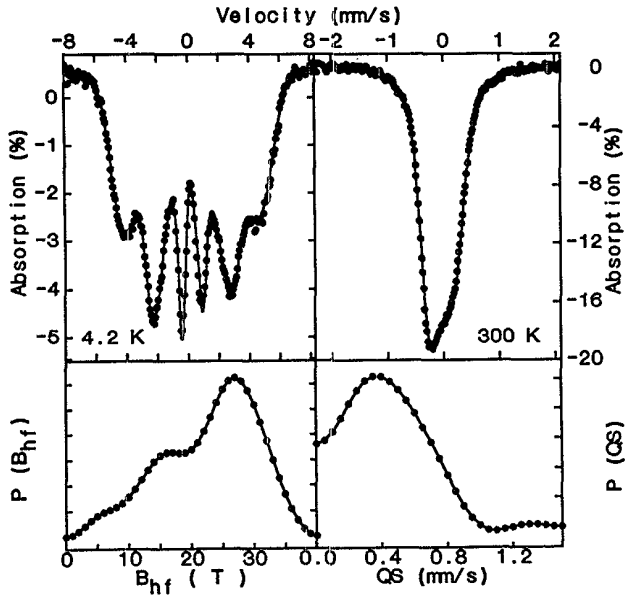

FIG. 3. Typical Mössbauer spectra of a-$Fe_{90}Sc_{10}$ measured at 4.2 K and 300 K. The fitted distributions of the hyperfine field (B_{hf}) and quadrupole splitting (Δ) are also shown.

TABLE I. Summary of the magnetic properties of a-Fe_xSc_{100-x}. Results refer to data at 4.2 K, except for the magnetic ordering temperature T_c and crystallization temperature T_x. Values in brackets in the $\langle B_{hf}\rangle$ column are deduced total iron moments in μ_B. See the text for explanation.

x (at. %)	T_c (K)	M_z (μ_B/Fe)	M_∞ (μ_B/Fe)	$\langle B_{hf}\rangle$ (T)	M_r (μ_B/Fe)	$\mu_0 H_c$ (mT)	T_x (K)
89	103	1.02	1.58	22.9 (1.53)	0.53		844
90	105	0.85	1.74	22.9 (1.53)	0.36	120	822
91	104	0.71	1.63	22.2 (1.48)	0.30	150	807

obtained by extrapolating the segment of the magnetization curves between 2 and 6 T to $\mu_0 H = 0$, is a measure of the longitudinal component of the iron moment. The fact that M_z is much smaller than M_∞ or the moment deduced from $\langle B_{hf}\rangle$ clearly indicates an asperomagnetic structure[6] with large random transverse components of the iron atomic moment. The asperomagnetic structure may be modeled by a uniform random distribution of orientation of the iron moments, their directions lying within a cone of half-angle Ψ.

Low-field dc thermomagnetization traces (Fig. 5) show broad peaks at ~100 K for all three samples. In order to avoid any effects of an external field on the magnetic ordering, we employed two zero-field techniques to determine T_c: the temperature dependence of the iron hyperfine field [for $x = 91$, Fig. 6(a)] and the temperature dependence of the resonant γ absorption at zero velocity [Fig. 6(b)]. Both of these measurements give magnetic ordering temperatures of about 100 K (values listed in Table I), and the transition in zero field is remarkably sharp, occurring within a few degrees, in contrast to the transition in an applied field. It should be noted that in the other amorphous alloys discussed here, there is a substantial gap between the onset of magnetic ordering and the appearance of a moment on all of the iron atoms, perhaps as much as 100 K.[3,11]

Hydrogen charging converts all of the alloys into collinear ferromagnets, with ordering temperatures of ~310 K (Table II). Magnetization curves at 4.2 K saturate easily in fields of order 100 mT (Fig. 7), so M_z is practically indistinguishable from M_∞, and deduced moments are in agreement with those obtained from the average hyperfine field (Table I). The coercivity measured at 4.2 K is also reduced, from ~120 to ~1 mT after hydrogenation.

DISCUSSION

The possibility that pure amorphous iron may exist in a number of distinct forms is a subject for speculation. Ryan and Coey[1] initially suggested that there may be more than one variety, on the basis of extrapolating magnetic measurements on several a-Fe_xM_{100-x} systems, while Xiao and Chien[2] found from room-temperature Mössbauer measurements that $\langle\Delta\rangle$ appeared to extrapolate to different values as $x \geq 100$, depending on whether M was an early transition metal or a metalloid, implying that structurally distinct forms of pure amorphous iron might exist. Subsequent work on a-$Fe_x(Nd, B)_{100-x}$ at elevated temperatures[20] extended this latter work to much higher iron concentrations, and clearly showed that for $x > 80$ the composition of the alloying component was largely irrelevant and that only one structural form exists.

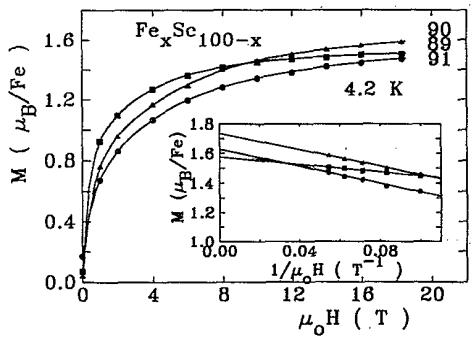

FIG. 4. Magnetization curves at 4.2 K for a-Fe_xSc_{100-x} ($x = 89, 90, 91$). The insert shows the moment per iron extrapolated to $1/H = 0$.

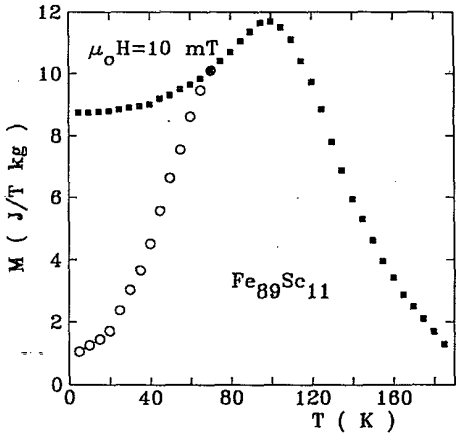

FIG. 5. Thermomagnetic curve for a-$Fe_{90}Sc_{10}$ in a field of 10 mT. ■, field-cooled and ○, zero-field cooled.

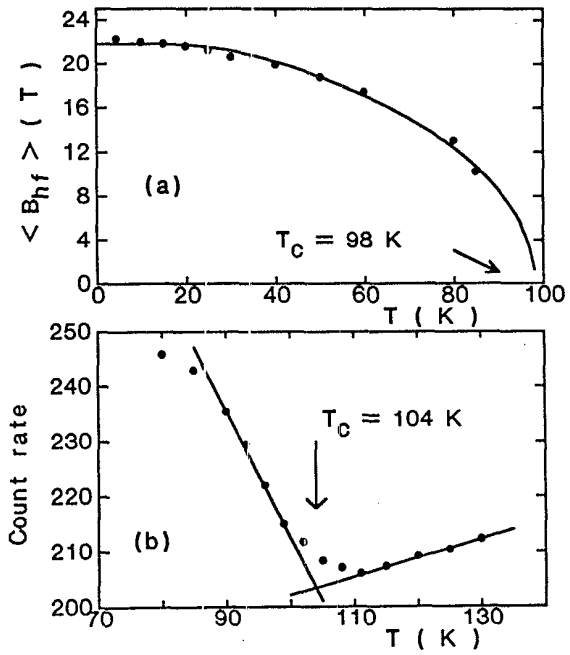

FIG. 6. (a) $\langle B_{hf}\rangle$ and (b) count rate at zero velocity as functions of temperature for a-$Fe_{91}Sc_9$.

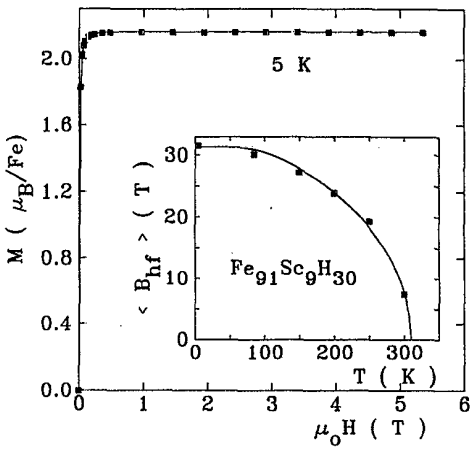

FIG. 7. Magnetization curve for a-$Fe_{91}Sc_9H_{30}$ at 4.2 K. Inset shows the temperature dependence of $\langle B_{hf}\rangle$.

Our Mössbauer experiments give parameters for a-Fe_xSc_{100-x} which are comparable to those of other early transition-metal systems. But the magnetic properties of this group of materials are not all alike. Data on four iron-rich alloys of similar composition are shown in Table III.

Iron-rich amorphous alloys with group IIIb elements (Sc and Y) are magnetically similar. They are asperomagnets, exhibiting a single spin-freezing transition at about 100 K. The equivalent alloys with elements from group IVb (Zr and Hf) also have an asperomagnetic ground state, but the magnetization curve approaches saturation more readily, as indicated by the ratio $M(5\ \mathrm{T})/M_\infty$ in Table III. They show higher-ordering temperatures, and there is a second transition at lower temperatures T_{xy}, where the transverse components of the moments freeze.[10]

These different ordering behaviors may be rationalized in terms of the distributed exchange Heisenberg spin-glass model of Gabay and Toulouse.[21] Figure 8 is a magnetic phase diagram based on this model, showing ordering temperatures as functions of concentration x and the average exchange (J) and the normalized width of the exchange distribution (J_0), which may include both positive (ferromagnetic) and negative (antiferromagnetic) values. The magnetic behavior of a-Fe_xM_{100-x} alloys may now be plotted.

For group IVb elements (track 1), magnetic orders first appear for $x \sim 35$ as a moment develops on the iron atom; at this point they are spin glasses ($\Psi = 180°$) with $J/J_0 < 1$. As x increases, J/J_0 rises rapidly and they enter a region where they exhibit two magnetic transitions; magnetic ordering sets in at progressively higher temperatures. As x increases the cone half-angle Ψ, decreases to zero and by $x \approx 50$ they are ferromagnetic, with $J/J_0 \gg 1$. Further addition of iron then leads only to an increase in T_c, but for $x > 85$, T_c starts to fall again and noncollinearity reappears because of a reduction of J/J_0 due to recurrence of antiferromagnetic exchange. Finally, a transverse spin-freezing transition T_{xy} appears below T_c, and by $x = 93$ in a-Fe-Zr, the two transitions have merged into a single spin-freezing transition at about 150 K.

Amorphous iron-based alloys with group IIIb exhibit only a single transition for all $x > 35$, where the iron moment first appears (track 2). They are asperomagnets with values of Ψ which decrease as the iron content rises, reaching a value of about 80° in a-$Fe_{88}Y_{12}$, and in the

TABLE II. Magnetic properties of hydrogenated a-$Fe_xSc_{100-x}H_y$. Results refer to data at 4.2 K, except for the magnetic ordering temperature (T_c). Value in brackets in the $\langle B_{hf}\rangle$ column is the deduced total iron moment (see the text).

x (at. %)	y (at. %)	T_c (K)	M_z (μ_B/Fe)	$\langle B_{hf}\rangle$ (T)	$\mu_0 H_c$ (mT)
89	30	>300	2.30		0.5
90	34	>300	2.22		0.8
91	29	~310	2.16	31.3 (2.09)	0.8

TABLE III. Comparison of amorphous iron-rich asperomagnetic alloys showing radius of alloying element (r), magnetic ordering temperature (T_c), average iron hyperfine field $\langle B_{hf} \rangle$, and the ratio between the magnetization in 5 T and extrapolated to $B_0 = \infty$.

Alloy	r (nm)	T_c (K)	$\langle B_{hf} \rangle$ (T)	$\frac{M(5\text{ T})}{M_{(\infty)}}$	Reference
$Fe_{90}Sc_{10}$ melt spun	0.162	105	22.9	0.75	this work
$Fe_{88}Y_{12}$ sputtered	0.178	109	30.1	0.76	11 and 12
$Fe_{90}Zr_{10}$ melt spun	0.160	226	25.5	0.92	8
$Fe_{90}Hf_{10}$ melt spun	0.167	233	25.9	0.96	9

present a-Fe-Sc alloys. The bias towards collinearity indicates the presence of substantial amounts of positive exchange, but the absence of a second transition at all compositions means that J/J_0 remains close to 1 for all x.

As expected from this model, both groups approach a common limit as $x \rightarrow 100$ and the effects of the different alloying elements are reduced. We predict that pure amorphous iron will exhibit a single magnetic transition to a speromagnetic spin structure, somewhere in the range 100–150 K.

It is far from clear that a local moment, mean-field model is the most appropriate choice as a description of the magnetic properties of a transition-metal glass, where the moments are associated with d -bands close to E_F and the dominant source of magnetic coupling is nearest-neighbor direct exchange. The moments in these alloys do possess a strong localized character, as can be seen from the coexistence of magnetic and nonmagnetic iron in alloys close to $x = 40$,[1,22] and this may in part be due to the static disorder present in amorphous alloys, but an infinite ranged view of the exchange is almost certainly invalid. We therefore do not claim that this model gives a complete description of magnetic order in these alloys, but rather that it provides a useful guide to the interpretation of the data. Furthermore, we have reported significant differences between the details of the observed and predicted behavior at both T_c and T_{xy},[3,10] which arise because the mean-field approximation inevitably misses local fluctuations. Despite its obvious shortcomings, it is the best model available.

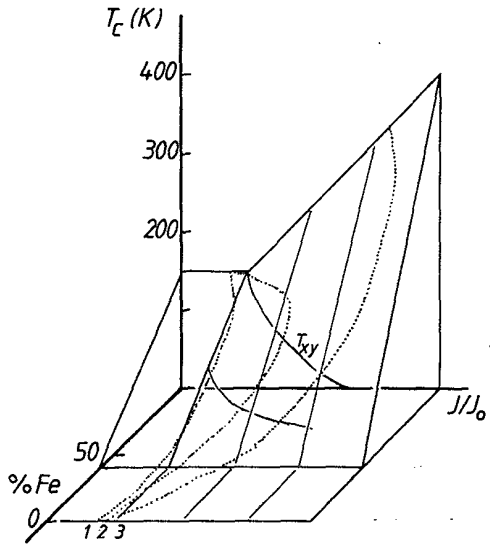

FIG. 8. Magnetic phase diagram for a-Fe_xM_{100-x} alloys (schematic) based on the model of Gabay and Toulouse (Ref. 22). Track 1 represents the path taken for M=Sc or Y. Track 2 represents the path taken for M=Zr or Hf. Track 3 is for any of the hydrogenated alloys.

The difference between alloys with group IIIb and IVb elements is not simply a reflection of atom size (see Table III), unlike the case of amorphous rare-earth iron alloys.[23] This suggests that there must be additional antiferromagnetic exchange in a-Fe-Y and a-Fe-Sc, which maintains the asperomagnetic order against the direct Fe-Fe ferromagnetic exchange. In *crystalline* Y and Sc there is evidence[24,25] that both hosts carry oscillating exchange between magnetic solutes, and that the same coupling persists in amorphous alloys.[26] It may be that the same mechanism is responsible for the additional exchange in our alloys; in this context it is worth noting that there is no evidence of Zr or Hf acting in the same way.

The reappearance of asperomagnetic order in the group IVb alloy series above $x = 85$, and its persistence in the group IIIb series for all iron concentrations, requires a further source of antiferromagnetic exchange. Here it is the distance dependence of iron-iron nearest-neighbor exchange which is known both experimentally[27] and theoretically[28] to change sign at ~0.25 nm. Since this is just twice the metallic radius of iron, contacts of this separation may be expected in a dense random-packed assembly of iron atoms, leading inevitably to antiferromagnetic exchange. As the alloying elements are removed, these short nearest-neighbor contacts become the dominant source of negative coupling, and a common end point for all of the alloy series is expected.

Hydrogen acts in two ways to reduce negative exchange and convert noncollinear alloys into ferromagnets with enhanced ordering temperatures. In iron-rich alloys it acts mainly by dilating the lattice, increasing iron-iron distances and thus reducing the incidence of antiferromagnetic coupling that results from short bonds. Hydrogen absorption in a-Fe-M alloys occurs almost entirely through the formation of H-M bonds, iron having almost no affinity for hydrogen. These bonds reduce the Fe-M interactions in the alloy, and the hydrogen screens the iron atoms from the effects of the alloying element.

Indeed, hydrogenation has been demonstrated to significantly reduce the critical iron concentration for moment formation in *a*-Fe-Y (Ref. 29) and *a*-Fe-Zr (Ref. 30) by reducing the hybridization of the Fe and *M d* -bands, which leads to the loss of the iron moment. In midrange alloys ($50 \leq x \leq 85$), hydrogen eliminates the differences between alloys with group IIIb and IVb elements, which are due solely to the alloying elements (it cannot, of course, affect differences due to local ordering or structure) by screening out the effects of the *M* atoms. In alloys with group IIIb elements it reduces long-range exchange, increasing J/J_0, and leads to ferromagnetic ordering. It should be noted that simply enhancing the strength of the Fe-Fe interactions independent of their signs cannot produce these effects, as this will only increase the ordering temperature without affecting the nature of the magnetic order; J/J_0 must be changed to achieve a change in magnetic structure. The hydrogenated alloys of any of the early transition metals follow track 3 on Fig. 8.

Finally, the origin of the difference between the results of Fukamichi *et al.*[14] on the one hand, and those of Day *et al.*[13] and the present work on the other, must be addressed. The samples in the first study were prepared by dc high-rate sputtering, but the differences are unlikely to be a reflection of preparation method: sputtered, melt-spun, and mechanically alloyed *a*-Fe-Zr alloys show essentially the same properties.[31] Fukamichi's alloys were sputtered onto Cu substrates, which were subsequently dissolved in an acid solution, and we have found that such treatment introduces hydrogen into *a*-Fe-Y alloys. Hydrogenation has a profound effect on the magnetic properties of *a*-Fe-*M* alloys in general,[3,8,9,15] and in particular *a*-Fe-Sc, as we have already shown; it increases both the magnetization and T_c and could therefore account for the differences between the sputtered and melt-spun samples. To check our hypothesis we have measured the magnetization curves of samples of *a*-$Fe_{90}Sc_{10}$ subjected to various acid etching treatments. Some typical results at both room temperature and 8 K are shown in Fig. 9. Simple acid etches were observed to have a profound effect on both the shape of the magnetization loop and the maximum magnetization obtained. The introduced hydrogen converts the alloys from asperomagnets to ferromagnets. Using oxidizing acids, e.g., HNO_3 or adding strong oxidizing agents (e.g., $KMnO_4$) to the etch bath reduced but did not eliminate the absorption of hydrogen. Curiously, the bath used by Fukamichi *et al.* [H_2SO_4 with CrO_3 (Ref. 14)] caused a greater change in the magnetic properties than the simple acid etch. During etching, free hydrogen forms directly on the surface of the material, which has such a strong affinity for hydrogen that an oxidizing agent cannot prevent significant absorption by the alloy. We therefore conclude that the differences in reported magnetic properties are artifacts of the improper sample handling and not of fundamental origin. This situation is reminiscent of some early work on rare-earth intermetallics where reduction of atmospheric water vapor produced samples of varying hydrogen content and so different magnetic properties.[32]

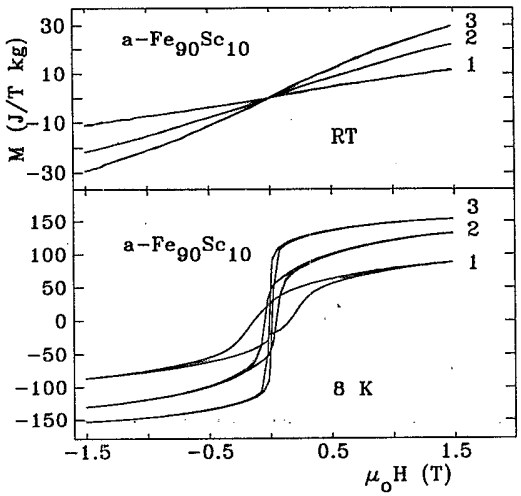

FIG. 9. Magnetization curves for *a*-$Fe_{90}Sc_{10}$ at room temperature and 8 K showing the effects of etching. 1, As made alloy; 2, etched 30 s in 10% H_2SO_4; 3, etched 30 s in bath used in Ref. 14.

CONCLUSIONS

Iron-rich Fe-Sc glasses are asperomagnetic. They exhibit a single magnetic transition at about 100 K, and the average iron moment, deduced from Mössbauer spectroscopy and high-field magnetization measurements, is 1.6 μ_B.

The sharp asperomagnetic ordering transition in zero applied field is peculiar to this system. All other alloys exhibiting this form of ordering have shown broad transitions which extend over as much as 100 K, or $\Delta T/T_c \sim 0.3$.

The addition of hydrogen transforms the alloys into ferromagnets with $T_c \sim 310$ K and iron moments of $2.2\mu_B$. All of these effects may be understood in terms of competing positive and negative exchange as described by Heisenberg spin-glass models.

Amorphous Fe_xM_{100-x} alloys exhibit rather different magnetic behavior according to whether *M* belongs to group IIIb (Sc, Y) or IVb (Zr, Hf); this is due mainly to the persistence of long-range exchange coupling in the former series of alloys.

All series of alloys tend to a common limit as $x \geq 100$, and pure amorphous iron is predicted to be speromagnetic below a single spin-freezing transition in the range 100–150 K.

ACKNOWLEDGMENTS

We are grateful to James Gavigan for collecting the high-field magnetization data at the Service National des Champs Intenses, Grenoble, and to Jacqueline Allan and Brian Buckley for help with some of the other measurements. This work was supported in part by a grant from the Natural Science and Engineering Research Council of Canada.

*Present address: The University of New South Wales, P.O. Box 1, Kensington, NSW 2033, Australia.

[1]J. M. D. Coey and D. H. Ryan, IEEE Trans. Magn. **MAG-20**, 1278 (1984).

[2]G. Xiao and C. L. Chien, Phys. Rev. B **35**, 8763 (1987).

[3]D. H. Ryan, in *Magnetic Properties of Amorphous Metals,* edited by A. Hernando, V. Madurga, M. C. Sanchez-Trujillo, and M. Vazquez (Elsevier, Amsterdam, 1987), p. 244.

[4]K. M. Unruh and C. L. Chien, J. Magn. Magn. Mater. **31–34**, 1587 (1983).

[5]S. M. Liou, G. Xiao, J. N. Taylor, and C. L. Chien, J. Appl. Phys. **57**, 3536 (1985).

[6]K. Moorjani and J. M. D. Coey, *Magnetic Glasses* (Elsevier, Amsterdam, 1984).

[7]H. Hiroyoshi and K. Fukamichi, Phys. Lett. **85A**, 242 (1981); J. Appl. Phys. **53**, 2226 (1982).

[8]D. H. Ryan, J. M. D. Coey, E. Batalla, Z. Altounian, and J. O. Ström-Olsen, Phys. Rev. B **35**, 8630 (1987).

[9]D. H. Ryan, J. M. D. Coey, and J. O. Ström-Olsen, J. Magn. Magn. Mater. **67**, 148 (1987).

[10]D. H. Ryan, J. O. Ström-Olsen, R. Provencher, and M. Townsend, J. Appl. Phys. **64**, 5787 (1988).

[11]J. M. D. Coey, D. Givord, A. Liénard, and J. P. Rebouillat, J. Phys. F **11**, 2707 (1981).

[12]J. Chappert, J. M. D. Coey, A. Liénard, and J. P. Rebouillat, J. Phys. F **11**, 2727 (1981).

[13]R. K. Day, J. B. Dunlop, C. P. Foley, M. Ghafari, and H. Pask, Solid State Commun. **56**, 843 (1985).

[14]K. Fukamichi, H. Hiroyshi, K. Shirakawa, T. Masumoto, and T. Kaneko, IEEE Trans. Magn. **MAG-22**, 424 (1986).

[15]J. M. D. Coey, A. Liénard, J. P. Rebouillat, D. H. Ryan, Wang Zhenxi, and Yu Boliang, J. Phys. F **18**, 1299 (1988).

[16]O. Kubaschewski, *Iron-Binary Phase Diagrams* (Springer-Verlag, Berlin, 1982).

[17]J. M. Coey, D. H. Ryan, and Yu Boliang, J. Appl. Phys. **55**, 1800 (1984).

[18]D. H. Ryan and J. M. D. Coey, J. Phys. E **19**, 693 (1986).

[19]P. C. M. Gubbens, J. H. F. van Appeldorn, A. M. van der Kraan, and K. H. J. Buschow, J. Phys. F **4**, 921 (1974).

[20]D. H. Ryan, L. X. Liao, and Z. Altounian, Solid State Commun., **66**, 339 (1988).

[21]M. Gabay and G. Toulouse, Phys. Rev. Lett. **47**, 201 (1981).

[22]J. Chappert, R. Arrese-Boggiano, and J. M. D. Coey, J. Magn. Magn. Mater. **7**, 175 (1978).

[23]N. Heiman and N. Kazama, Phys. Rev. B **19**, 1623 (1979).

[24]H. Nagasawa and T. Sugawara, J. Phys. Soc. Jpn. **23**, 711 (1967); L. L. Isaacs, Phys. Rev. B **8**, 3301 (1973); K. Baberschke, P. Pureur, A. Fert, R. Wendler, and S. Senoussi, *ibid.* **29**, 4999 (1984).

[25]B. V. B. Sarkissian and B.R. Coles, Commun. Phys. **1**, 17 (1976); L. E. Wenger, G. W. Hunter, J. A. Mydosh, J. A. Gotaas, and J. J. Rhyne, Phys. Rev. Lett. **56**, 1090 (1986); J. A. Gotaas, J. J. Rhyne, L. E. Wenger, and J. A. Mydosh, J. Appl. Phys. **63**, 3577 (1988).

[26]J. Durand and S. J. Poon, J. Phys. (Paris) Colloq. **40**, C5-231 (1979).

[27]W. Kümmerle and U. Gradmann, Solid State Commun. **24**, 33 (1977).

[28]C. S. Wang, B. M. Klein, and H. Krakauer, Phys. Rev. Lett. **54**, 1852 (1985); F. J. Pinski, J. Staunton, B. L. Gyoffy, D. D. Johnson, and G. M. Stocks, *ibid.* **56**, 2096 (1986).

[29]D. H. Ryan, J. M. Cadogan, E. J. Devlin, and J. M. D. Coey, Z. Phys. Chem. Neue Folge **145**, 113 (1985).

[30]S. M. Fries, C. L. Chien, J. Crummenauer, H. G. Wagner, and U. Gonser, J. Less-Common Met. **130**, 17 (1987).

[31]C. Michaelsen and E. Hellstern, J. Appl. Phys. **62**, 117 (1987).

[32]W. E. Wallace, in *Hydrogen in Metals I,* edited by G. Alefeld and J. Völkl (Springer-Verlag, Berlin, 1978), Chap. 7, p. 169.